Tools for Studying Aqueous Enantioselective Lanthanide-Catalyzed Mukaiyama Aldol Reactions

82x31mm (96 x 96 DPI)

Catalysis Science & Technology

MINIREVIEW

Tools for Studying Aqueous Enantioselective Lanthanide-Catalyzed Mukaiyama Aldol Reactions

Derek J. Averill and Matthew J. Allen[*]

Enantioselective bond-forming reactions catalyzed by chiral lanthanide-based complexes are popular because of their Lewis acidity, solvent compatibility, reusability, and potential to catalyze reactions with high stereospecificity. The stereospecific outcomes of bond-forming reactions catalyzed by asymmetric lanthanide-based precatalysts depend on the coordination chemistry of the precatalysts that can be interrogated with X-ray crystal structures, luminescence measurements, NMR spectroscopy, and computational methods. This review is primarily focused on developments related to lanthanide-based precatalysts since the turn of the century and the techniques used to study coordination environments of lanthanide-based precatalysts for Mukaiyama aldol reactions in aqueous media.

Introduction

The trivalent lanthanide ions (Ln^{3+}) are of great importance due to their photophysical properties, Lewis acidity, stability in aqueous media (hydrolysis constants between 7.6 and 8.5 and water-exchange rate constants greater than 6×10^7), and reusability.[1] Because of these features, Ln^{3+}-based precatalysts are popular alternatives to moisture-sensitive Lewis acids such as $AlCl_3$, $TiCl_4$, $SnCl_4$, and $SiCl_4$.[2] In select cases, Ln^{3+} ions can be combined with chiral ligands to form enantioselective precatalysts for bond-forming reactions.[3] The improvement of chiral, Ln-based precatalysts is limited by the need to understand reaction pathways and key precatalyst features such as metal-complex stability and coordination geometry. Toward this goal, spectroscopic measurements and computational studies have been used to unveil reaction pathways and precatalyst stabilities for carbon–carbon bond-forming reactions. This minireview is focused on developments reported since the turn of the century and is composed of five parts: (1) development of enantioselective, water-tolerant, lanthanide-based precatalysts for Mukaiyama aldol reactions; (2) crystal structure determination of precatalysts; (3) luminescence measurements to study Eu^{3+}-based precatalysts; (4) ^{1}H-NMR experiments to study Ln^{3+}-based precatalysts; and (5) computational studies of Mukaiyama aldol reactions. Comprehensive reviews that describe older work, non-lanthanide precatalysts, or reactions other than Mukaiyama aldol can be found elsewhere.[4]

Part 1: Development of enantioselective, water-tolerant, lanthanide-based precatalysts for Mukaiyama aldol reactions.

The Ln^{3+}-catalyzed Mukaiyama aldol reaction is of great interest to synthetic chemists because it is a water-tolerant, carbon–carbon bond-forming reaction that can produce β-hydroxy carbonyls (Scheme 1), which are important functional groups found in and used to synthesize many biologically active compounds.[5] Further, the

reaction can be carried out in aqueous media, and high enantiomeric ratios can be achieved with the use of chiral precatalysts.[3a–d,6] Recovery and reuse of Ln^{3+}-based precatalysts has been demonstrated with no significant loss of reactivity, making Ln^{3+}-based precatalysts a topic of study for sustainable chemistry applications.[7]

Scheme 1. Example of a Ln^{3+}-catalyzed Mukaiyama aldol reaction.
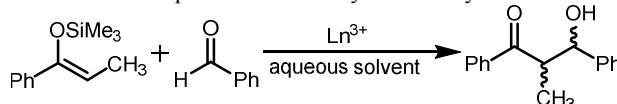
To date, several ligands have been synthesized to prepare enantioselective, water-tolerant, Ln^{3+}-based precatalysts for Mukaiyama aldol reactions.[3a–c,8] The two most effective ligands reported are hexadentate with two nitrogen and four oxygen donor atoms.[3a,c] Although ligands **1** and **2** are hexadentate and have the same donor atoms, they have different donor functional groups and are structurally different (Figure 1).
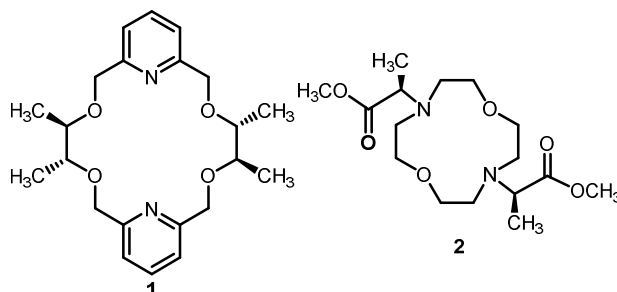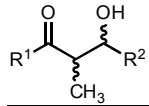

Figure 1. Chiral ligands used for lanthanide-catalyzed, water-tolerant, enantioselective Mukaiyama aldol reactions.[3a,c]

Precatalysts formed from lanthanide triflate salts using ligands **1** and **2** promote reactions that result in a range of stereospecific β-hydroxy carbonyl compounds.[3a,c] Mukaiyama aldol reactions promoted by either ligands **1** or **2** with $Ln(OTf)_3$ have a wide range of reactivities

This journal is © The Royal Society of Chemistry 2013

Catal. Sci. Technol., 2014, 00, 1-3 | 1

and selectivities. Ligand **1** with either $Ce(OTf)_3$ or $Pr(OTf)_3$ catalyzes a variety of Mukaiyama aldol reactions to produce different products (Table 1) with diastereomeric ratios (dr, *syn*:*anti*) ranging from 90:10 to 95:5 and enantiomeric ratios (er, *R/S*) ranging from 87.5:12.5 to 91.5:8.5 (Table 1). Ligand **2** with either $Eu(OTf)_3$ or $Nd(OTf)_3$ catalyzes Mukaiyama aldol reactions with diastereoselectivities (*syn*:*anti*) ranging from 75:25 to 97.3:2.7 and enantioselectivities (*R/S*) ranging from 82:18 to 98:2.

**Table 1.** Aqueous enantioselective Mukaiyama aldol reaction results.

R^1	R^2	Ln^{3+}	ligand	dr^h	er (*syn*)	ref
Ph	Ph	Ce^{3+a}	1^c	93:7	91:9	4f
Ph	$4\text{-}CH_3OC_6H_4$	Pr^{3+b}	1^d	92:8	87.5:12.5	3b
Ph	$2\text{-}CH_3OC_6H_4$	Pr^{3+b}	1^d	95:5	91.5:8.5	3b
Ph	$4\text{-}ClC_6H_4$	Pr^{3+b}	1^d	90:10	91.5:8.5	3b
Ph	1-naphthyl	Pr^{3+b}	1^d	91:9	90.5:9.5	3b
Ph	Ph	Eu^{3+a}	2^e	97:3	96.5:3.5	3c
Ph	$4\text{-}ClC_6H_4$	Eu^{3+a}	2^e	95:5	95.5:4.5	3c
Ph	$4\text{-}CH_3C_6H_4$	Eu^{3+a}	2^e	96:4	95:5	3c
Ph	$(CH_2)_5CH_3$	Eu^{3+a}	2^e	96:4	98:2	3c
Ph	Ph	Nd^{3+a}	2^c	75:25	82:18	3d
Ph	Ph	Nd^{3+a}	2^f	95:5	95.6:4.4	3d
Ph	Ph	Nd^{3+a}	2^g	97:3	96:4	3d
$4\text{-}ClC_6H_4$	Ph	Nd^{3+a}	2^g	94:6	96:4	3d
$4\text{-}CH_3C_6H_4$	Ph	Nd^{3+a}	2^g	97:3	96:4	3d
Ph	$4\text{-}ClC_6H_4$	Nd^{3+a}	2^g	92:8	95:5	3d
Ph	$4\text{-}CH_3C_6H_4$	Nd^{3+a}	2^g	97:3	96:4	3d

^{a}20 mol %, ^{b}10 mol %, ^{c}24 mol %, ^{d}12 mol %, ^{e}48 mol %, ^{f}36 mol %, ^{g}42 mol %, ^{h}(*syn*:*anti*)

An important feature of the Ln^{3+} series is the steady decrease in ionic radii from La^{3+} (103.2 pm) to Lu^{3+} (86.1 pm). This feature of the Ln^{3+} series was explored to identify the best suited Ln^{3+} ion to combine with ligands **1** or **2**.[3a,d] In a benchmark Mukaiyama aldol reaction (Scheme 2), ligand **1** with Ce^{3+} and ligand **2** with Nd^{3+} produced the highest enantioselectivites. With both ligands, small changes in Ln^{3+} size drastically affect reaction outcomes in terms of selectivity (Figure 2 and Table 2). By comparison of selectivity with Ln^{3+} ionic radius, lanthanide complexes of ligand **1** appear to have smaller binding pockets than those of ligand **2**, likely contributing to differences in selectivity based on substrate bulk.

Scheme 2. Ln^{3+}-catalyzed Mukaiyama aldol reaction used to monitor selectivity with precatalysts that use ligands **1** or **2**.
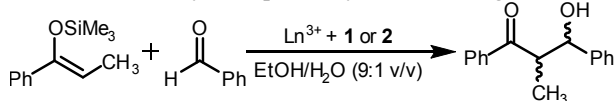
Although high enantio- and diastereoselectivities can be observed for the water-tolerant Mukaiyama aldol reaction using Ln^{3+} ions with ligands **1** or **2**, reaction times are long and high ligand loadings are required.[3a-d] These limitations have prompted investigations of the Ln^{3+}-based precatalysts to learn more about the structure of the precatalysts and the mechanism of the reaction. Due to the labile nature of Ln^{3+} complexes in aqueous media, details about Ln^{3+}–ligand and substrate–

precatalyst interactions and transition state models likely will assist in future developments of Ln^{3+}-based precatalysts.
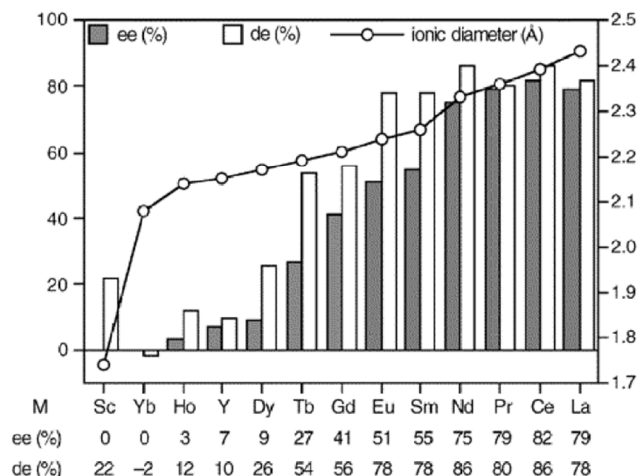

Figure 2. Graph of selectivity data for the reaction shown in Scheme 2 using different Ln^{3+} ions and ligand **1**. Increased selectivity is observed as the ionic diameters of Ln^{3+} increase from Yb^{3+} to Ce^{3+}. Adapted with permission from S. Kobayashi, T. Hamada, S. Nagayama and K. Manabe, *Org. Lett.*, 2001, **3**, 165. Copyright 2001 American Chemical Society.

Table 2. Selectivity data for the reaction shown in Scheme 2 using different Ln^{3+} ions with ligand **2**. Selectivity is highest for ligand **2** and Nd^{3+}. A ligand-to-Ln^{3+} ratio of 1.2:1 was used instead of 2.4:1 so that a difference in selectivity could be observed for the different Ln^{3+} with ligand **2**.[3d]

Ln^{3+}	Ln^{3+} radius (pm)	*syn*:*anti*	er (*syn*)
La^{3+}	103.2	1.7:1	52:48
Ce^{3+}	102	1.8:1	60:40
Pr^{3+}	99	2.2:1	74:26
Nd^{3+}	98.3	3.0:1	82:18
Sm^{3+}	95.8	2.1:1	58:42
Eu^{3+}	94.7	2.4:1	75:25
Gd^{3+}	93.8	2.7:1	74:26
Tb^{3+}	92.3	2.5:1	72:28
Dy^{3+}	91.2	2.0:1	64:36
Ho^{3+}	90.1	1.9:1	59:41
Er^{3+}	89.0	1.8:1	58:42
Tm^{3+}	88.0	1.5:1	53:47
Yb^{3+}	86.8	1.3:1	50:50
Lu^{3+}	86.1	1.4:1	51:49

Part 2: Crystal structure determination of precatalysts.

X-ray crystal structures are useful for determining relative orientation of ligands that surround Ln^{3+} ions and information related to ligand–metal interactions,[3a,9] even though they do not necessarily reflect the structure in solution. A crystal structure of ligand **1** with $Pr(NO_3)_3$ (Figure 3) was solved, and it was found that Pr^{3+} and **1** bind in a 1:1 ligand-to-metal stoichiometry and that Pr^{3+} is nearly in the plane of the ring. Although NO_3^- anions were not used in Mukaiyama aldol reactions with **1** and Pr^{3+}, NO_3^- anions might have aided in the formation of crystals for analysis. Further, the structure revealed that the methyl groups are in the axial positions, likely forcing the stereochemical outcomes of reactions performed with this precatalyst.

2 | *Catal. Sci. Technol.*, 2014, **00**, 1-3 1-3

This journal is © The Royal Society of Chemistry 2012

Despite not being used in the Mukaiyama aldol reaction, the pre-catalyst in Figure 4 was used in the nitroaldol reaction and studied using X-ray crystallography.[3e,9b] Ligand-to-metal binding stoichiometries and geometries of a chiral Tb^{3+}-containing complex were studied by solving crystal structures in the presence of excess citrate, lactate, glycinate, and serinate anions.[9b] The information gained from these structures was helpful in thinking about how the pre-catalyst reacts with solvent, substrates, and products during the reaction. In general, crystal structures are helpful for the development of precatalysts because they enable rational modifications to the geometry of precatalysts by changing ligands that surround the metal center.
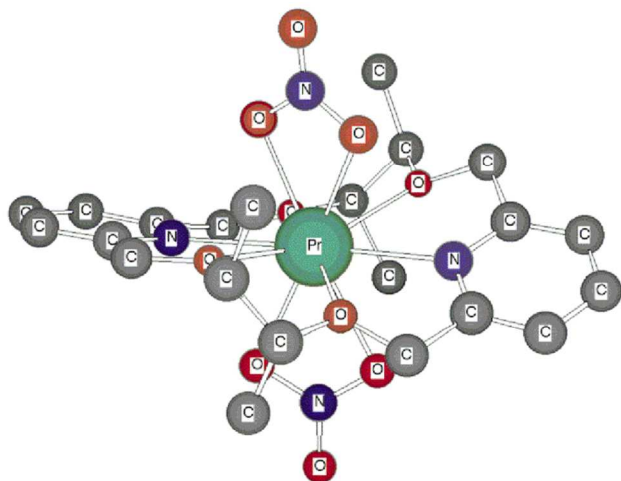

Figure 3. X-ray crystal structure of $[Pr(NO_3)_2 \cdot \mathbf{1}]^+$. Hydrogen atoms have been omitted for clarity. Reprinted with permission from S. Kobayashi, T. Hamada, S. Nagayama and K. Manabe, *Org. Lett.*, 2001, **3**, 165. Copyright 2001 American Chemical Society.
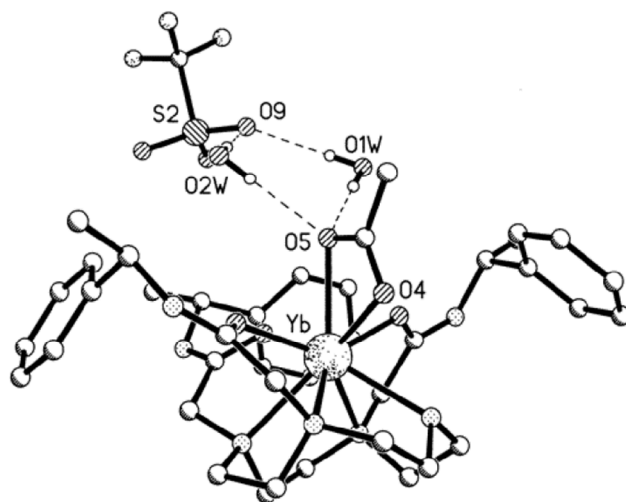

Figure 4. X-ray crystal structure of Yb^{3+}-based precatalyst showing a distant triflate anion and chelated acetate moiety with its hydrogen bonding interactions to nearby water molecules. The macrocycle is 1,4,7,10-tetraazacyclododecane, and it has methyl and phenyl substitutions on its three pendant amide sidearms that are coordinated to Yb^{3+}. Reprinted with permission from R. S. Dickins, S. Aime, A. S. Batsanov, A. Beeby, M. Botta, J. I. Bruce, J. A. K. Howard, C. S. Love, D.

Parker, R. D. Peacock and H. Puschmann, *J. Am. Chem. Soc.*, 2002, **124**, 12697. Copyright 2002 American Chemical Society.

Part 3: Luminescence measurements to study Eu^{3+}-based precatalysts.

A widely used technique to study the number of metal-bound water molecules (q) of contrast agents for magnetic resonance imaging was adapted to study Eu^{3+}-based precatalysts in aqueous media.[10] The technique is based on a series of empirically derived equations, similar to eq 1, that were derived by measuring the differences of luminescence-decay rates of crystalline Eu^{3+}-containing complexes with known q values.[11] Inner-sphere oscillators other than water are accounted for with correction constants where n_{OH} is the number of inner-sphere alcoholic O–H oscillators, n_{NH} is the number of inner-sphere amine N–H oscillators, and $n_{O=CNH}$ is the number of inner-sphere amide N–H oscillators. The uncertainty of this equation is ±0.1 water molecules.[11a] A detailed review of the derivation and theory of these equations can be found elsewhere.[12]

$$q = 1.11[\tau_{H_2O}^{-1} - \tau_{D_2O}^{-1} - 0.31 + 0.45 n_{OH} + 0.99 n_{NH} + 0.075 n_{O=CNH}] \qquad (1)$$

To gain mechanistic insight into the aqueous Ln^{3+}-catalyzed Mukaiyama aldol reaction, eq 1 was used to calculate the number of Eu^{3+}-bound water molecules at different stages of the catalytic cycle of the Mukaiyama aldol reaction (Scheme 3). The study was carried out in mixtures of tetrahydrofuran (THF) and water. THF was chosen as a cosolvent because it does not have O–H or N–H oscillators that would complicate the measurements. By presynthesizing the reaction product, the coordination environment of Eu^{3+} was studied in four different scenarios: (1) $Eu(OTf)_3$ with no starting materials; (2) $Eu(OTf)_3$ with silyl enol ether; (3) $Eu(OTf)_3$ with benzaldehyde; and (4) $Eu(OTf)_3$ with product. Values of q were calculated for Eu^{3+} in all four scenarios. The water-coordination number calculations revealed that benzaldehyde displaced coordinated water. Furthermore, the ability to displace water changes as a function of solvent composition. Additionally, neither the silyl enol ether nor the product was able to displace Eu^{3+}-coordinated water molecules, and consequently, product inhibition is not likely to occur for the reaction in question. These results provide mechanistic details about the aqueous lanthanide-catalyzed Mukaiyama aldol reaction and a route to study other reactions that use Eu^{3+}-based precatalysts.

Scheme 3. Proposed aqueous lanthanide triflate-catalyzed Mukaiyama aldol catalytic cycle. Adapted with permission from P. Dissanayake and M. J. Allen, *J. Am. Chem. Soc.*, 2009, **131**, 6342. Copyright 2009 American Chemical Society.
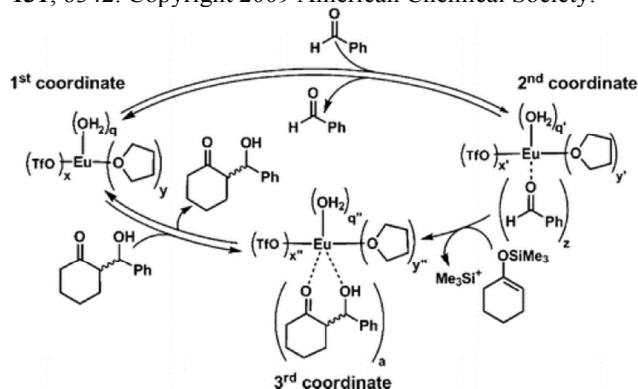
By measuring q and monitoring rates of Mukaiyama aldol reactions that use either $Eu(OTf)_3$ or $Eu(NO_3)_3$ precatalysts in solvent systems containing between 1 and 40% H_2O in THF (Scheme 4), it was

This journal is © The Royal Society of Chemistry 2012

Catal. Sci. Technol., 2014, **00**, 1-3 | 3

found that reactivity increases with increased q (as a general trend, q increases with water concentration for $Eu(NO_3)_3$ and $Eu(OTf)_3$) for Eu^{3+}-based precatalysts (Figure 5).[13] This discovery is important because future Eu^{3+}-based precatalysts can be designed in a way that maximizes their reactivity by taking advantage of ligand features such as denticity and electron donating ability.

To gain insight into factors that affect the selectivity and reactivity of Ln^{3+}-based precatalysts, six variations of ligand **2** were combined with Eu^{3+} (Figure 6).[3c] Luminescence-decay measurements were used to study changes of q (Δq) of ligand–Eu^{3+} systems in the absence and presence of benzaldehyde. Additionally, reactivities of each precatalyst were compared by differences in isolated yields and enantiomeric ratios were determined by chiral high performance liquid chromatography analyses (Table 3).

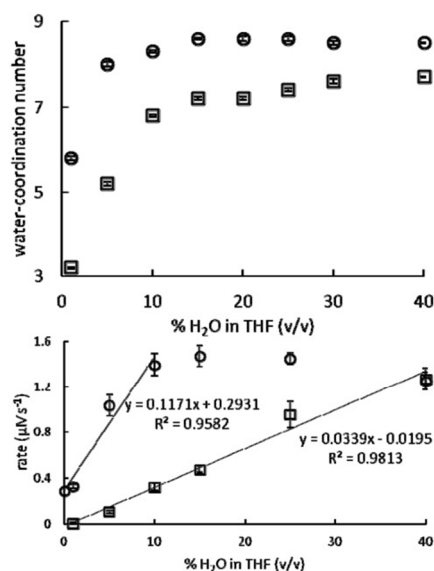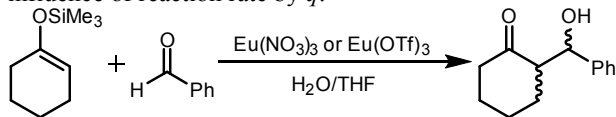**Scheme 4.** Mukaiyama aldol reaction used to study the influence of reaction rate by q.[13]

Figure 5. Top, Water-coordination number of $Eu(OTf)_3$ (○), and $Eu(NO_3)_3$ (□) as a function of % H_2O in THF (v/v). Error is represented by standard error of the mean of between 3 and 9 measurements. Bottom, Steady-state reaction rates of 7 mol % $Eu(OTf)_3$- (○) or $Eu(NO_3)_3$-catalyzed (□) Mukaiyama aldol reactions in 0–40% H_2O in THF (v/v). Regression lines represent the dependence of rate on solvent composition and anion identity. Reprinted with permission from Averill, D. J.; Dissanayake, P.; Allen, M. J. The Role of Water in Lanthanide-Catalyzed Carbon–Carbon Bond Formation. Molecules 2012, 17, 2073–2081. http://www.mdpi.com/1420-3049/17/2/2073.

Yields for Mukaiyama aldol reactions catalyzed by ligands **2–5** with Eu^{3+} were high (>80%) while ligands **6–8** with Eu^{3+} had low yields (≤20%).[3c] These results indicate that complexes with a greater propensity to exchange coordinated water for benzaldehyde, Δq, (Figure 7) are more reactive than complexes that are less influenced by benzaldehyde. Additionally, ligands **6** and **7** with branched ester groups (R = i-Pr or t-Bu) gave low yields. These results are likely related to the reduced chance of benzaldehyde displacing Eu^{3+}-coordinated water. Surprisingly, Eu^{3+} and ligand **8** (R = H) resulted in a low yield (8%) and a Δq

of only −0.09. The reduction in reactivity and Δq are likely due to differences in Lewis acidity of the Eu^{3+}-containing complexes caused by the carboxylic acid sidearms of **8** vs the ester sidearms of ligands **2–7**. Enantioselectivity was not observed for **8** with Eu^{3+} and that is not surprising because there is no bulky "R" group to selectively block incoming nucleophiles (Figure 8). Based on q and selectivity data, for selectivity to occur in Mukaiyama aldol reactions catalyzed by ligands **2–8** with Eu^{3+}, the ester sidearm must block the incoming nucleophilic attack.
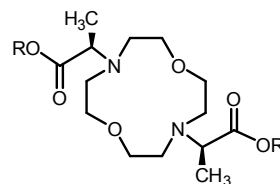
ligand	**2**	**3**	**4**	**5**	**6**	**7**	**8**
R	CH_3	C_2H_5	n-C_3H_7	n-C_4H_9	i-Pr	t-Bu	H

Figure 6. Hexadentate ligands used to study changes in selectivity and reactivity based on ligand identity.

Table 3. Selectivity, reactivity, and coordination changes among different Eu^{3+}-based precatalysts using the ligands from Figure 6.[3c] Larger absolute values of Δq indicate larger changes in water coordination number.
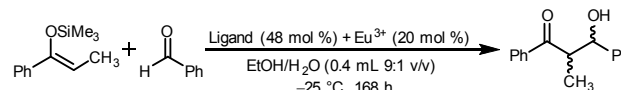
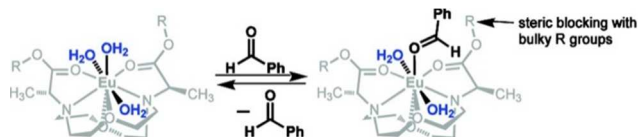| ligand	Δq	yield (%)	er (*syn*)
2	−0.68	92	96.5:3.5
3	−0.40	82	92.5:7.5
4	−0.45	83	93:7
5	−0.49	83	93.5:6.5
6	−0.19	20	90:10
7	−0.14	18	75.5:24.5
8	−0.09	8	0

Figure 7. Proposed equilibrium leading to the activation and selective nucleophilic attack of benzaldehyde. Adapted with permission from Y. Mei, P. Dissanayake and M. J. Allen, *J. Am. Chem. Soc.*, 2010, **132**, 12871. Copyright 2010 American Chemical Society.
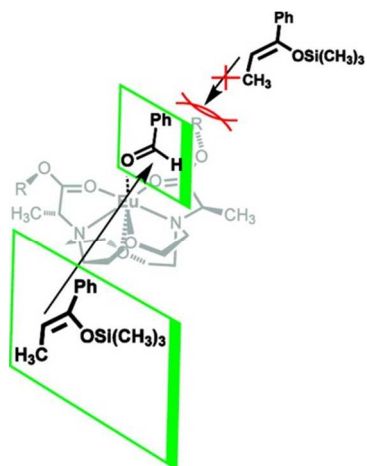
4 | *Catal. Sci. Technol.*, 2014, **00**, 1-3 1-3

This journal is © The Royal Society of Chemistry 2012

Figure 8. Proposed transition state for the asymmetric Mukaiyama aldol reaction using hexadentate ligands **2**–**8** and Eu^{3+} as a precatalyst. Reprinted with permission from Y. Mei, P. Dissanayake and M. J. Allen, *J. Am. Chem. Soc.*, 2010, **132**, 12871. Copyright 2010 American Chemical Society.

To investigate changes in relative Eu^{3+} binding strengths as a function of chiral center location, bulk, and sidearm donor type (ester, carboxylic acid, alcohol, and amide), the interactions between six hexadentate ligands (Figure 9) and Eu^{3+} were studied using luminescence-decay measurements.[8b] Water-coordination numbers were measured at different ligand-to-metal ratios (Table 4), and it was found that Eu^{3+} is coordinatively saturated (Figure 10) in the presence of excess hexadentate ligands ($q = 0$). By comparing q data with yields, it was concluded that binding Eu^{3+} with hexadentate ligands likely slows Mukaiyama aldol reactions. These observations are in agreement with earlier studies,[3a,13] and they are helpful for the future design of water-tolerant enantioselective Ln^{3+}-based precatalysts because ligands must minimize unbound Ln^{3+} while avoiding deactivation of Ln^{3+}.
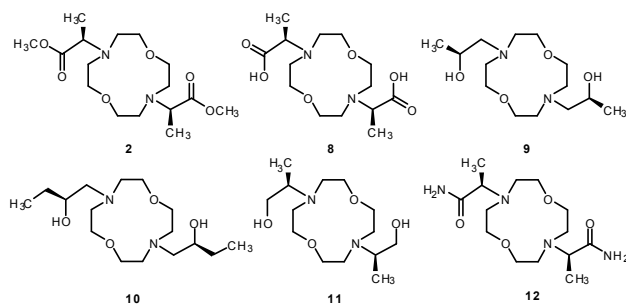

Figure 9. Hexadentate ligands studied in the presence of Eu^{3+}.[8b]

Steady-state luminescence measurements can be used as a supplemental technique to q measurements for the rapid (seconds) analysis of changes in Eu^{3+} coordination environments.[1d,1e,4a,4b] Eu^{3+} emission spectra can be highly sensitive to changes in coordination environment (Figure 11). Therefore, luminescence measurements can be used to study changes in Eu^{3+} coordination environments. Comparison of the $^5D_0{\rightarrow}^7F_1$ (~591 nm) and $^5D_0{\rightarrow}^7F_2$ (~616 nm) transitions of Eu^{3+} is a useful tool for the ratiometric monitoring ligand-to-Eu^{3+} titrations.[14] Ligand-to-Eu^{3+} titrations were monitored by plotting the ratio of Eu^{3+} emission intensity at 616 nm divided by the emission intensity at 591 nm [$(^5D_0{\rightarrow}^7F_2)/(^5D_0{\rightarrow}^7F_1)$] as a function of ligand-to-metal ratio for ligands **2** and **8**–**12** (Figure 12). Steady-state luminescence measurements do not provide q values, but they enable monitoring changes in

coordination environment by avoiding the need to obtain luminescence-decay rates in deuterated solvent systems. Steady-state luminescence measurements were found to be a useful tool for studying changes in Eu^{3+} coordination during ligand-to-Eu^{3+} titrations.

Table 4. Water-coordination numbers[a] for Eu^{3+} with ligands **2** and **8**–**12**.[8b]

ligand	$q^{b,c}$	$q^{b,d}$	$q^{c,e}$	$q^{d,e}$	$q^{c,f}$	$q^{d,f}$
2[g]	3.5	3.5	2.1	2.1	1.4	1.4
8[g]	2.2	2.2	0.8	0.8	0.0	0.0
9	2.2	1.1	2.0	1.0	1.1	0.0
10	1.9	0.8	1.8	0.8	nd	nd
11	2.1	1.0	2.1	1.0	0.5	0.0
12	3.8	3.4	3.0	2.6	1.7	1.3

[a]The error associated with water-coordination number determination is ±0.1 water molecules. [b]Ligand-to-metal ratio of 1:1. [c]Calculated for complexes with Eu^{3+} coordination by one ligand. [d]Calculated for complexes with Eu^{3+} coordination by two ligands. [e]Ligand-to-metal ratio of 2:1. [f]Ligand-to-metal ratio of 6:1. [g]Ligands **1** and **2** do not have chelator-based inner-sphere O–H or N–H oscillators; therefore, $q^c = q^d$. nd = not determined.
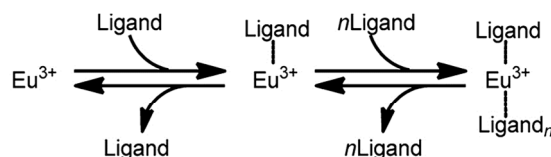
fast but not selective   slow and selective   no reaction

Figure 10. Proposed equilibria involving multiple Eu^{3+} species. Reprinted with permission from D. J. Averill and M. J. Allen, *Inorg. Chem.*, 2014, **53**, 6257. Copyright 2014 American Chemical Society.
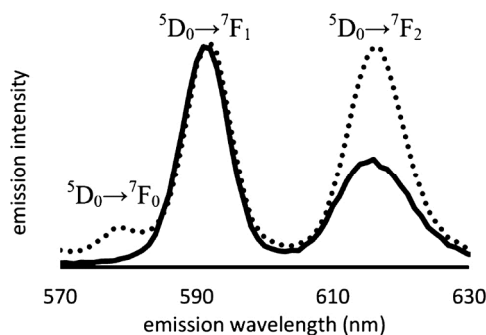

Figure 11. Emission spectra of $Eu(OTf)_3$ in 9:1 $EtOH/H_2O$ with (dotted line) and without (solid line) a hexadentate ligand. Adapted with permission from D. J. Averill and M. J. Allen, *Inorg. Chem.*, 2014, **53**, 6257. Copyright 2014 American Chemical Society.

Figure 12. Emission intensity ratios of Eu^{3+} (616 nm/591 nm) versus equivalents of ligand for Eu^{3+} with **2** (△), **8** (▲), **9** (◆), **10** (◇), **11** (○), and **12** (□). Increases in magnitude of the emission intensity quotient (616 nm/591 nm) arise from perturbations in the crystal field splitting of Eu^{3+}. Adapted with permission from D. J. Averill and M. J. Allen, *Inorg. Chem.*, 2014, **53**, 6257. Copyright 2014 American Chemical Society.
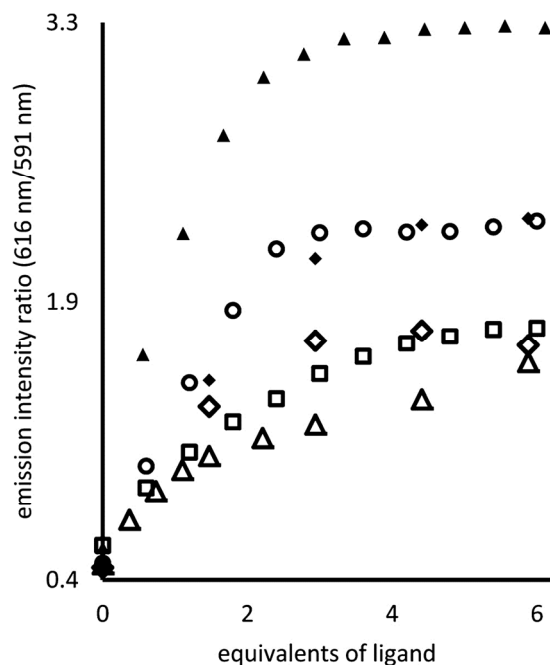
Part 4: ^{1}H-NMR experiments to study Ln^{3+}-based precatalysts.

In addition to Eu^{3+} luminescence measurements for the study of structural features of Ln^{3+}-based precatalysts, ^{1}H-NMR studies have been used.[3a,e,8b] Changes in ligand environment can be found by monitoring ^{1}H-NMR spectra of ligands in the absence of Ln^{3+} and presence of varying amounts of Ln^{3+}. Kobayashi and co-workers used ^{1}H-NMR studies to investigate ligand **1** in the presence of $La(OTf)_3$. By changing ligand-to-metal stoichiometries and comparing ^{1}H-NMR spectra, they found that ligand **1** binds to La^{3+} tightly (only scarce amounts of free **1** were observed in the ^{1}H-NMR spectra).[3a] From ^{1}H-NMR experiments, it was found that at least three distinct species can exist in solution when Eu^{3+} is combined with ligands **2** and **8**–**12** (Figure 13) and the ratio of these species is influenced by ligand-to-Eu^{3+} ratios.[8b] The findings are important because Le Chatelier's principle can be followed to drive the equilibria towards selective precatalysts (one hexadentate ligand per Ln^{3+} ion). ^{1}H-NMR experiments provide valuable information about ligand environments that complement Eu^{3+} luminescence measurements.
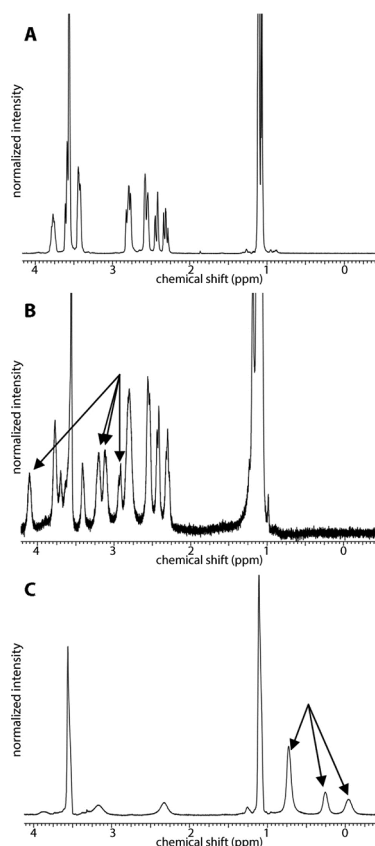
Figure 13. (A) ^{1}H-NMR spectrum of **9** in 9:1 $EtOD/D_2O$. (B) ^{1}H-NMR spectrum of **9** in 9:1 $EtOD/D_2O$ at –40 °C with 0.25 equiv of $Eu(OTf)_3$. Arrows point to signals observed in the presence of excess ligand (the temperature of –40 °C was required to resolve the signals between 4 and 2 ppm). These new signals are attributed to a Eu^{3+}–L_n ($n > 1$) species. (C) ^{1}H-NMR spectrum of **9** in 9:1 $EtOD/D_2O$ with 2 equiv of $Eu(OTf)_3$. Arrows point to signals observed in the presence of excess Eu^{3+}. The new upfield signals are attributed to Eu^{3+}_n–L ($n \geq 1$) species. Adapted with permission from D. J. Averill and M. J. Allen, *Inorg. Chem.*, 2014, **53**, 6257. Copyright 2014 American Chemical Society.

Part 5: Computational studies of Mukaiyama aldol reactions.

Computational studies of Ln^{3+}-catalyzed Mukaiyama aldol reactions can provide details about the reaction mechanism that are not readily accessible by X-ray crystal structures, luminescence measurements, or NMR experiments. Recently, Morokuma and co-workers reported two computational studies that are based on the reaction in Scheme 4.[15] The studies were focused on transition states of the reaction to learn about diastereoselectivity and the changes in free energy of Eu^{3+} complexes depending on coordination environment. To study transition states of Mukaiyama aldol reactions, the Morokuma group used a computational technique called artificial force-induced reaction to explore approximate reaction pathways that start from dissociation limits or local minima.[15a] By studying the C–C–C–O dihedral angles (ϕ), they found that the reaction shown in Scheme 4 may have as many as 17 different transition states that are within 2 kcal/mol of each other (Table 5). It is worth noting that four of the five most likely transition states are for reactions that result in *syn* products. The authors suggest

that this small energy difference for transition states leads to the low diastereoselectivity of Mukaiyama aldol reactions.

Table 5. Relative free energies, key structural parameters, and existence probability of lower transition states, with ΔΔG less than 2 kcal/mol.[15a]

transition states	ΔΔG (kcal/mol)	ϕ (deg)	product	existence probability (%)
1	0.00	180.6	*syn*	20.85
2	0.28	180.6	*syn*	12.94
3	0.40	53.1	*anti*	10.59
4	0.45	49.0	*syn*	9.73
5	0.85	161.3	*syn*	4.96
6	0.86	180.2	*syn*	4.89
7	0.97	55.0	*syn*	4.02
8	1.16	298.2	*syn*	2.92
9	1.27	51.2	*anti*	2.46
10	1.28	174.5	*anti*	2.41
11	1.28	291.1	*anti*	2.41
12	1.28	176.0	*anti*	2.38
13	1.30	178.1	*syn*	2.32
14	1.44	166.4	*syn*	1.84
15	1.56	59.2	*syn*	1.50
16	1.58	161.6	*syn*	1.44
17	1.73	182.9	*anti*	1.12

In addition to investigating factors that affect selectivity of Mukaiyama aldol reactions, the Morokuma group studied factors that affect reactivity.[15b] By dissecting the reaction into fragments (Figure 14), they were able to calculate the free energy of transition states that are likely to take place during the course of the reaction (Figure 15). These results are helpful because they help predict minimum energy pathways. The Morokuma group reported that the reaction begins with a Eu^{3+}-coordinated benzaldehyde followed by C–C bond formation between the silyl enol ether and the coordinated aldehyde. They calculated that a series of proton transfers occurs after the C–C bond formation and finally the silyl group dissociates after nucleophilic attack from a water molecule as shown in Figure 15. The computational studies reviewed here contribute to the further understanding of factors that influence rates and selectivity of Mukaiyama aldol reactions. Studies of this nature can be used in the future to aid in the development of selective catalysts for Ln^{3+}-catalyzed bond forming reactions.
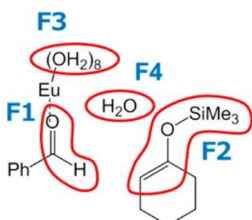
Figure 14. Fragments F1, F2, F3, and F4 used by Morokuma and co-workers to study the Mukaiyama aldol reaction by the artificial force-induced reaction method. Reprinted with permission from M. Hatanaka and K. Morokuma, J. Am. Chem. Soc., 2013, 135, 13972. Copyright 2013 American Chemical Society.

Figure 15. Reaction pathway as calculated by the artificial force-induced reaction method. Reprinted with permission from M. Hatanaka and K. Morokuma, J. Am. Chem. Soc., 2013, 135, 13972. Copyright 2013 American Chemical Society.
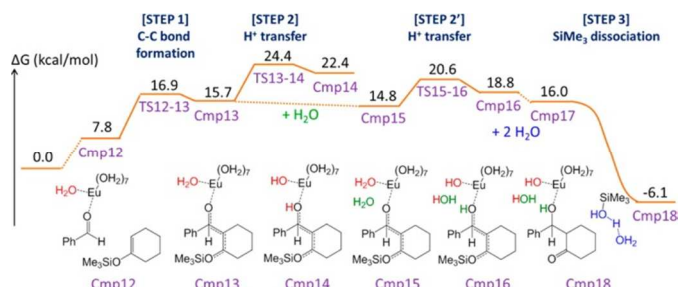
Conclusions

Since the turn of the century the pursuit of highly efficient water-tolerant Ln^{3+}-based precatalysts has led to stunning results. Recent developments have made the study of Ln^{3+}-based precatalysts more accessible, and tools like luminescence and NMR spectroscopy have made these developments possible. Further development of water-tolerant Ln^{3+}-based precatalysts is essential because these precatalysts have the ability to be recovered and reused if implemented properly.

Acknowledgements

Notes and references

Department of Chemistry, Wayne State University, Detroit, MI 48202, USA. E-mail: mallen@chem.wayne.edu

1 (a) K. Ouchi, S. Saito and M. Shibukawa, *Inorg. Chem.*, 2013, **52**, 6239; (b) F. Caillé, C. S. Bonnet, F. Buron, S. Villette, L. Helm, S. Petoud, F. Sezenet and É. Tóth, *Inorg. Chem.*, 2012, **51**, 2522; (c) C. M. Andolina, R. A. Mathews and J. R. Morrow, *Helv. Chim. Acta*, 2009, **92**, 2330; (d) G. R. Choppin and Z. M. Wang, *Inorg. Chem.* 1997, **36**, 249; (e) M. J. Lochhead, P. R. Wamsley and K. L. Bray, *Inorg. Chem.* 1994, **33**, 2000; (f) W. D. Horrocks, Jr. and D. R. Sudnick, *J. Am. Chem. Soc.*, 1979, **101**, 334; (g) S. L. Wu and W. D. Horrocks, Jr., *Inorg. Chem.*, 1995, **34**, 3724; (h) I. Sánchez-Lombardo, C. M. Andolina, J. R. Morrow and A. K. Yatismirsky, *Dalton Trans.*, 2010, **39**, 864; (i) S. Kobayashi and I. Hachiya, *Tetrahedron Lett.*, 1992, **33**, 1625; (j) S. Kobayashi and I. Hachiya, *J. Org. Chem.*, 1994, **59**, 3590; (k) S. Kobayashi, S. Nagayama and T. Busujima, *J. Am. Chem. Soc.*, 1998, **120**, 8287; (l) T. Kitanosono and S. Kobayashi, *Adv. Synth. Catal.*, 2013, **355**, 3095.

2 (a) Y. Miyahara and Y. N. Ito, *J. Org. Chem.*, 2014, **79**, 6801; (b) M. Rigo, P. Canu, L. Angelin and G. D. Valle, *Ind. Eng. Chem. Res.* 1998, **37**, 1189; (c) I. Kulszewicz-Bajer, A. Proń, J. Abramowicz, C. Jeandey, J.-L. Oddou and J. W. Sobczak, *Chem. Mater.*, 1999, **11**, 552; (d) S. E. Denmark and J. R. Heemstra, Jr., *Org. Lett.*, 2003, **5**, 2303.

3 (a) S. Kobayashi, T. Hamada, S. Nagayama and K. Manabe, *Org. Lett.*, 2001, **3**, 165; (b) T. Hamada, K. Manabe, S. Ishikawa, S. Nagayama, M. Shiro and S. Kobayashi, *J. Am. Chem. Soc.*, 2003,

125, 2989; (c) Y. Mei, P. Dissanayake and M. J. Allen, *J. Am. Chem. Soc.*, 2010, **132**, 12871; (d) Y. Mei, D. J. Averill and M. J. Allen, *J. Org. Chem.* 2012, **77**, 5624; (e) S. U. Pandya, R. S. Dickens and D. Parker, *Org. Biomol. Chem.*, 2007, **5**, 3842; (f) J. R. Robinson, X. Fan, J. Yadav, P. J. Carroll, A. J. Wooten, M. A. Pericàs, E. J. Schelter and P. J. Walsh, *J. Am. Chem. Soc.*, 2014, **136**, 8034; (g) G. Desimoni, G. Faita, F. Piccinini and M. Toscanini, *Eur. J. Org. Chem.*, 2006, 5228.

4 (a) F. S. Richardson, *Chem. Rev.*, 1982, **82**, 541; (b) J.-C. G. Bünzli and C. Piguet, *Chem. Soc. Rev.*, 2005, **34**, 1048; (c) S. B. J. Kan, K. K.-H. Ng and I. Paterson, *Angew. Chem. Int. Ed.*, 2013, **52**, 9097; (d) J. Mlynarski and J. Paradowska, *Chem. Soc. Rev.*, 2008, **37**, 1502; (e) S. Kobayashi, M. Sugiura, H. Kitagawa and W. W.-L. Lam, *Chem. Rev.*, 2002, **102**, 2227; (f) S. Kobayashi and K. Manabe, *Acc. Chem. Res.* 2002, **35**, 209; (g) S. Kobayashi and C. Ogawa, *Chem. Eur. J.*, 2006, **12**, 5954; (h) T. Kitanosono, T. Ollevier and S. Kobayashi, *Chem. Asian J.*, 2013, **8**, 3051.

5 (a) Y. Lee, J. Y. Choi, H. Fu, C. Harvey, S. Ravindran, W. R. Roush, J. C. Boothroyd and C. Khosla, *J. Med. Chem.*, 2011, **54**, 2792; (b) M. Tosin, L. Smith and P. F. Leadlay, *Angew. Chem. Int. Ed.*, 2011, **50**, 11930; (c) M. Morar, K. Pengelly, K. Koteva and G. D. Wright, *Biochemistry*, 2012, **51**, 1740; (d) J. W. Park, H.-S. Oh, W. S. Jung, S. R. Park, A. R. Han, Y.-H. Ban, E. J. Kim, H.-Y. Kang and Y. J. Yoon, *Chem. Commun.*, 2008, 5782; (e) A. P. Green, A. T. L. Lee and E. J. Thomas, *Chem. Commun.*, 2011, **47**, 7200; (f) H.-S. Oh and H.-Y. Kang, *J. Org. Chem.*, 2012, **77**, 1125.

6 (a) S. Kobayashi, S. Nagayama and T. Busujima, *Chem. Lett.*, 1999, 71; (b) S. Kobayashi, S. Nagayama and T. Busujima, *Tetrahedron*, 1999, **55**, 8739; (c) S. Nagayama and S. Kobayashi, *J. Am. Chem. Soc.*, 2000, **122**, 11531; (d) T. Ollevier and B. Plancq, *Chem. Commun.*, 2012, **48**, 2289.

7 (a) Y. S. Kim, S. Matsunaga, J. Das, A. Sekine, T. Ohshima and M. Shibasaki, *J. Am. Chem. Soc.*, 2000, **122**, 6506; (b) K. Mikami, Y. Mikami, H. Matsuzawa, Y. Matsumoto, J. Nishikido, F. Yamamoto and H. Nakajima, *Tetrahedron*, 2002, **58**, 4015.

8 (a) J. S. Bradshaw, P. Huszthy, C. W. McDaniel, C. Y. Zhu, N. K. Dalley and R. M. Izatt, *J. Org. Chem.*, 1990, **55**, 3129; (b) D. J. Averill and M. J. Allen, *Inorg. Chem.*, 2014, **53**, 6257.

9 (a) T. Harada, H. Tsumatori, K. Nishiyama, J. Yuasa, Y. Hasegawa and T. Kawai, *Inorg. Chem.*, 2012, **51**, 6476; (b) R. S. Dickins, S. Aime, A. S. Batsanov, A. Beeby, M. Botta, J. I. Bruce, J. A. K. Howard, C. S. Love, D. Parker, R. D. Peacock and H. Puschmann, *J. Am. Chem. Soc.*, 2002, **124**, 12697.

10 P. Dissanayake and M. J. Allen, *J. Am. Chem. Soc.*, 2009, **131**, 6342.

11 (a) R. M. Supkowski and W. D. Horrocks, Jr., *Inorg. Chim. Acta*, 2002, **340**, 44; (b) A. Beeby, I. M. Clarkson, R. S. Dickens, S. Faulkner, D. Parker, L. Royle, A. S. de Sousa, J. A. G. Williams and M. Woods, *J. Chem. Soc., Perkin Trans. 2*, 1999, 493; (c) P. Dissanayake, Y. Mei and M. J. Allen, *ACS Catal.* 2011, **1**, 1203.

12 Z. Lin and M. J. Allen, *Dyes Pigments*, 2014, **110**, 261.

13 D. J. Averill, P. Dissanayake and M. J. Allen, *Molecules*, 2012, **17**, 2073.

14 (a) G. Dehaen, G. Absillis, K. Driesen, K. Binnemans and T. N. Parac-Vogt, *Helv. Chim. Acta*, 2009, **92**, 2387; (b) M. P. Bemquerer, C. Bloch, Jr., H. F. Brito, E. E. S. Teotonio and M. T. M. Miranda, *Inorg. Biochem.*, 2002, **91**, 363.

15 (a) M. Hatanaka, S. Maeda and K. Morokuma, *J. Chem. Theory Comput.*, 2013, **9**, 2882; (b) M. Hatanaka and K. Morokuma, *J. Am. Chem. Soc.*, 2013, **135**, 13972.

8 | *Catal. Sci. Technol.*, 2014, **00**, 1-3 1-3

This journal is © The Royal Society of Chemistry 2012